Lithuanian Journal of Physics
Vol. **65**, No. 1, pp. 1–18 (2025)
ISSN 1648-8504 eISSN 2424-3647
DOI: https://doi.org/10.3952/physics.2025.65.1.3

NONLINEAR EXCITON EQUATION FACTORIZATION FOR NON-PERTURBATIVE ABSORPTION MODELLING

V. Bubilaitis and D. Abramavičius

Institute of Chemical Physics, Faculty of Physics, Vilnius University, Saulėtekio 3, 10257 Vilnius, Lithuania
Email: vytautas.bubilaitis@ff.vu.lt

Received 22 June 2024; revised 9 August 2024; accepted 5 September 2024

Various types of optical spectra of molecular systems are often analyzed via perturbative series expansion in the powers of optical field. The simplest absorption is related to the linear optical response. However, observed spectral features can be mislabelled if higher orders are not vanishing. High-intensity excitation field breaks the established assumption of quickly converging perturbative regime. Non-perturbative quantum methods can solve these problems. However, they lead to endless hierarchies of equations that, in general, cannot be solved analytically. Dropping terms at a specific order or factorizing (expressing high-order terms as products of several lower-order terms) can be used to close the hierarchy. We propagate the nonlinear exciton equations (NEE) with exciton–exciton annihilation (EEA) non-perturbatively in a high-excitation regime and calculate absorption spectra of a molecular aggregate using various factorization schemes. The results demonstrate that the solution is weakly sensitive to the factorization method when EEA is included.

Keywords: non-perturbative, exciton–exciton annihilation, molecular aggregate, nonlinear exciton equations, factorization

1. Introduction

Laser excitation intensity in laser spectroscopy is often an overlooked parameter, which can be employed in a measurement primarily for improving the signal-to-noise ratio; however, at high intensities the spectrum may be affected by system nonlinearities. At weak excitation intensities, the signal analysis is usually performed in the perturbative regime [1]. In this regime, the number of quanta, participating in the specific processes, or the order of the processes in relation to the field can be explicitly counted, simplifying the overall analysis. However, at high orders to the field, various processes become indistinguishable, the perturbative series essentially fails to converge, and excitation-induced effects of different orders appear at various types of signals, which are usually associated with much lower order measurements (even as low as the first-order signals). This can lead to the misinterpretation of spectral features and thus requires a special non-perturbative treatment.

Non-perturbative methods generate endless hierarchies of equations that, in general, cannot be solved analytically [2]. Dropping terms at specific order or variable factorization (expressing high-order terms as products of several lower-order terms) is required to close the hierarchy. This can lead to unexpected results from equations, e.g. diverging solutions, giving nonphysical effects, or losing expected effects. However, as a positive feature, due to the high number of excitations, the factorized equations may lead to correct multi-quanta cumulative average spectral features which cannot be easily captured using perturbative regimes.

Exciton–exciton annihilation (EEA) [3–7] is a process that becomes apparent at a high excitation density in various molecular aggregates. This process involves at least two separate excitations creating a short-lived molecular double-excited state. The following nonradiative decay leads to the decay of one excitation and only one excitation remains. Accordingly, we must describe an effective nonlinear excitation density decay in the medium.

Due to the short lifetime of double excited states, the higher – triple or quadruple, etc. – excitations become impossible and, as a result, the equations describing such high-order resonances do not contribute to the result. As a result, the corresponding variables in the equations can be dropped or factorized.

We derive equations for non-perturbative calculations of the spectra of a set of coupled oscillators by using a nonlinear exciton equations (NEE) formalism. NEE generate the endless hierarchy of coupled equations. For the practical use, we apply specific assumptions that give a solid basis to ending the hierarchy at some well-defined level. By adding or deleting EEA terms we can reason about the number of excitations, which effectively can exist in the system. Following that, if we have terms that are related to a very high number of excitations, we factorize them and treat them as products of lower-order terms. Depending on a specific system of interest and a specific spectroscopic measurement, such factorization is not arbitrary, and some properties that are important may get lost. Hence, the systematic analysis of various factorization schemes is necessary. In this work, we compare several factorization types for a linear chromophore aggregate from low to high excitation field intensities by calculating the simplest possible absorption spectrum. We demonstrate that at a high excitation intensity, an additional induced absorption may be observed, while its characteristics are very sensitive to system nonlinearities and, hence, the type of factorization. This can be utilized in a specific application for a specific molecular system.

2. Theory of non-perturbative optical response using nonlinear exciton equations

2.1. Coherent dynamics of generalized quantum particles

We have used nonlinear exciton equations (NEE) [8, 9] to describe the pump-probe and two-dimensional electronic spectra of simple chromophore aggregates at various excitation conditions [5, 10, 11]. The NEE treats a chromophoric aggregate as a system of coupled nonlinear oscillators. The equations are obtained from the Frenkel exciton Hamiltonian on a lattice, forming a specific network:

$$\hat{H} = \sum_{m,n} J_{mn}\hat{b}_m^\dagger \hat{b}_n + \frac{1}{2}\sum_m K_m \hat{b}_m^{\dagger 2}\hat{b}_m^2 + \sum_m \mu_m^-(t)\hat{b}_m^\dagger + \sum_m \mu_m^+(t)\hat{b}_m. \quad (1)$$

Here the indices m, n label different oscillators (chromophores) positioned on different lattice sites. $\hat{b}_m^\dagger$ ($\hat{b}_m$) is the excitation creation (annihilation) operator for the oscillator m. The matrix J_{mn} defines the fundamental properties of the system: diagonal ($m = n$) matrix elements are fundamental excitation energies, and off-diagonal ($m \neq n$) matrix elements are hopping amplitudes (often denoted by resonant coupling). K_m is the mth oscillator anharmonicity. $\mu_m^\pm(t)$ are optical field-induced system–field interaction amplitudes, which are defined later – they are responsible for the excitation (and deexcitation) of the system by the external optical field. When the field is off, this Hamiltonian conserves the number of particles. Note that we set $\hbar = 1$, so that frequency and energy are interchangeable.

The system can be populated by a various number of excitations: only a single excitation is involved in a linear optical response, while up to five excitations can be created at the fifth order. This is traced by the polarization operator defined as

$$\hat{P} = \sum_n \mu_n \left(\hat{b}_n^\dagger + \hat{b}_n\right). \quad (2)$$

Here $\boldsymbol{\mu}_n$ is the transition dipole moment of nth oscillator. Multi particle behaviour is characterized by operator commutation relations. For paulions [12, 13] we would have $[\hat{b}_n,\hat{b}_m^\dagger]_P = \delta_{mn}(1 - 2\hat{b}_m^\dagger \hat{b}_n)$ and for bosons we would have $[\hat{b}_n,\hat{b}_m^\dagger]_B = \delta_{mn}$ (notice that the paulions have the same commutation properties as fermions; however, the excitons do not have a spin degree of freedom). Both models change excitation dynamics. Neither bosonic nor paulionic models are correct to properly characterize electronic excitations of molecular chromophores, where a molecular double excitation is usually possible, while its excitation amplitude does not follow a harmonic oscillator character as is the case for bosons. Hence, the molecules possess a highly anharmonic excitation level scheme with unique transition dipoles deviating significantly from the harmonic model of bosons or from the paulions. One way to take into account these properties is to add additional nonlinear terms

to the polarization operator [14]. Alternatively, the generalized commutation relation can be used:

$$[\hat{b}_n,\hat{b}_m^\dagger] = \delta_{mn}(1 - 2\eta\hat{b}_m^\dagger\hat{b}_n). \tag{3}$$

Here η can be considered as a tunable parameter, which goes from 0 to 1. The case of $\eta = 0$ corresponds to the boson case, while $\eta = 1$ to paulions. The intermediate case affects the energy anharmonicity and the double-excitation amplitude compared to the fundamental excitation and could be tuned to describe specific molecular electronic excitations.

Interaction of the system with the optical field in the dipole approximation is taken into account within the rotating wave approximation (RWA). We thus use the system–field coupling terms in the following form:

$$\mu_m^{\pm}(t) = \boldsymbol{\mu}_m \cdot \boldsymbol{E}(t - t_0)\exp(\pm i\omega_0(t - t_0)). \tag{4}$$

Here $\boldsymbol{\mu}_m$ is the transition dipole of oscillator m, $\boldsymbol{E}(t - t_0)$ is the optical electric field envelope function centred at time t_0, while the optical carrier frequency is ω_0.

Superpositions of excitations, which are eigenvectors of the Hamiltonian system within the single-excitation manifold, are denoted by excitons. Such eigenvalue equation is

$$\sum_n J_{m,n}\theta_{n,a} = E_{m,n}\theta_{n,a}\,. \tag{5}$$

Here $\theta_{m,a}$ are eigenvectors forming the eigenvector matrix (in columns), E_a is the corresponding eigenvalue, a is the index of the exciton, and m labels different oscillators.

The NEE is the set of equations that is obtained by applying the Heisenberg equation of motion for an arbitrary operator $\hat{A}$,

$$i\frac{d\hat{A}}{dt} = \left[\hat{A},\hat{H}\right], \tag{6}$$

in the Heisenberg picture starting from the polarization operator (essentially from the annihilation operators, see Eq. (2)). Notice that then all operators are time dependent, i.e. $\hat{b}_n \to \hat{b}_n(t)$; however, for shortening the notation from this point we imply their time dependence; however, we do not label that explicitly. Hence, the equation for the operator $\hat{b}_n$ involves the products $\hat{b}_m\,\hat{b}_n$, $\hat{b}_m^\dagger\,\hat{b}_n$, $\hat{b}_k^\dagger\,\hat{b}_m\hat{b}_n$, then we write equations for these products, etc., and this yields a hierarchy of equations [5], which is called NEE. Notice that the polarization operator involves the single optical transition. Therefore, a single optical interaction results in the creation or annihilation of an excitation (quanta), so following the number of interactions becomes directly related to the number of creation/annihilation operators in various terms. Additionally, various types of exciton–exciton interactions yield higher-order contributions to the lower-order terms. Hence, the b_n-related variable is at least the first order to the field, $\hat{b}_n\hat{b}_v$-related variable is at least the second order to the field, etc. Up to the fifth order to the field we find

$$i\frac{d\hat{b}_u}{dt} = J_{un}\hat{g}_u\hat{b}_n + (1-\eta)K_u\hat{b}_u^\dagger\hat{g}_u\hat{y}_{uu} + \mu_u^-(t)\hat{g}_u, \tag{7}$$

$$\begin{aligned} i\frac{d\hat{\sigma}_{uv}}{dt} &= J_{vn}\hat{b}_u^\dagger\hat{g}_v\hat{b}_n - J_{nu}\hat{b}_n^\dagger\hat{g}_u\hat{b}_v \\ &+ (1-\eta)K_v\hat{b}_u^\dagger\hat{\sigma}_{vv}\hat{b}_v - (1-\eta)K_u\hat{b}_u^\dagger\hat{\sigma}_{uu}\hat{b}_v \\ &+ \mu_v^-(t)\hat{b}_u^\dagger\hat{g}_v - \mu_u^+(t)\hat{g}_u\hat{b}_v, \end{aligned} \tag{8}$$

$$\begin{aligned} i\frac{d\hat{y}_{uv}}{dt} &= J_{vn}\hat{g}_v\hat{y}_{un} + J_{un}\hat{g}_u\hat{y}_{vn} - 2\eta\delta_{uv}J_{vn}\hat{g}_v\hat{y}_{vn} \\ &+ \mu_v^-(t)\hat{g}_v\hat{b}_u + \mu_u^-(t)\hat{g}_u\hat{b}_v - 2\delta_{uv}\eta\mu_v^-(t)\hat{g}_v\hat{b}_v \\ &+ (1-\eta)(K_v\hat{\sigma}_{vv} + K_v\hat{\sigma}_{uu})\hat{y}_{uv} \\ &+ (1-\eta)\delta_{uv}K_v(1-\eta(3-2\eta)\hat{\sigma}_{vv})\hat{y}_{vv}, \end{aligned} \tag{9}$$

$$\begin{aligned} i\frac{d\hat{z}_{kuv}}{dt} &= J_{vn}\hat{b}_k^\dagger\hat{g}_v\hat{y}_{un} + J_{un}\hat{b}_k^\dagger\hat{g}_u\hat{y}_{vn} \\ &- 2\eta\delta_{uv}J_{vn}\hat{b}_k^\dagger\hat{g}_v\hat{y}_{vn} - J_{mk}\hat{b}_m^\dagger\hat{g}_k\hat{y}_{uv} \\ &- \mu_k^+(t)\hat{g}_k\hat{y}_{uv} + \mu_v^-(t)\hat{b}_k^\dagger\hat{g}_v\hat{b}_u \\ &+ \mu_u^-(t)\hat{b}_k^\dagger\hat{g}_u\hat{b}_v - 2\eta\delta_{uv}\mu_v^-(t)\hat{b}_k^\dagger\hat{g}_v\hat{b}_v \\ &+ (1-\eta)\hat{b}_k^\dagger(K_v\hat{\sigma}_{vv} + K_u\hat{\sigma}_{uu} - K_k\hat{\sigma}_{kk})\hat{y}_{uv} \\ &+ (1-\eta)\delta_{uv}K_v\hat{b}_k^\dagger(1-\eta(3-2\eta)\hat{\sigma}_{vv})\hat{y}_{vv}, \end{aligned} \tag{10}$$

where on the right-hand side, the indices m and n are summed over the whole lattice. Here we also defined the composite operators $\hat{\sigma}_{uv} = \hat{b}_u^\dagger\hat{b}_v$, $\hat{y}_{uv} = \hat{b}_u\hat{b}_v$, $\hat{z}_{kuv} = \hat{b}_k^\dagger\hat{b}_u\hat{b}_v$ as well as $\hat{g}_u = (1 - 2\eta\hat{\sigma}_{uu})$. Since the operator $\hat{\sigma}_{uu}$ is the number operator, the operator $\hat{g}_u$ in NEE implies rescaling of Hamiltonian parameters due to pre-excitation. Notice that we maintain the properly ordered form for all

terms: $\hat{b}^\dagger_u\hat{g}_v\hat{b}_n = (\hat{\sigma}_{un} - 2\eta\hat{b}^\dagger_u\hat{b}^\dagger_v\hat{b}_v\hat{b}_n)$ and $\hat{b}^\dagger_k\hat{g}_v\,\hat{y}_{un} = (\hat{z}_{kun} - 2\eta\hat{b}^\dagger_k\hat{b}^\dagger_v\hat{b}_v\hat{b}_u\hat{b}_n)$.

The hierarchy of equations is endless [5]. However, truncating the hierarchy at a specific number of excitations becomes possible when the experiment under consideration is designed to detect a specific optical process.

The equations for operators can be implemented for numerical calculations by formally switching to operator expectation values. Taking an arbitrary system state $|\psi\rangle$, the expectation values of all operator combinations in NEE can be formally calculated and the operator products turn into numbers (and the hats are being dropped to denote the expectation values): $b_u(t) \equiv \langle\psi|\hat{b}_u|\psi\rangle$, $y_{uv}(t) \equiv \langle\psi|\hat{b}_u\hat{b}_v|\psi\rangle$, $\sigma_{uv}(t) \equiv \langle\psi|\hat{b}^\dagger_u\hat{b}_v|\psi\rangle$, $z_{kuv}(t) \equiv \langle\psi|\hat{b}^\dagger_k\hat{b}_u\hat{b}_v|\psi\rangle$ etc. Notice that the state $|\psi\rangle$ does not need to be specified explicitly, except for the vacuum state, where all variables vanish. The system is in the vacuum state before turning the optical field on, i.e. before the excitation and detection process. Starting from this state, equations can be propagated numerically or solved analytically. From practical considerations, in the following sections, we will drop from equations the terms that are higher than the fifth order in the optical field and include only up to two-quanta resonances.

2.2. Dephasing and relaxation

NEE for operators in Eqs. (7–10) do not include dephasing or relaxation. To properly describe these processes, it is required to take into account the surrounding phonon environment. Such are intramolecular vibrational degrees of freedom (local phonons), being inseparable companions of the chromophores. The phonons are harmonic oscillators linearly coupled to the sites. We assume that they induce only uncorrelated transition energy fluctuations, so the system–environment Hamiltonian is

$$\hat{H}_{\mathrm{SB}} = \frac{1}{2}\sum_m\sum_a L_{ma}\hat{b}^\dagger_m\hat{b}_m\hat{Q}_a + \mathrm{h.c.}, \tag{11}$$

where $\hat{Q}_a$ is the coordinate of αth phonon, and L_{ma} is the interaction strength for the energy fluctuations. Accordingly, the only nonzero correlation functions (in the interaction picture) are

$$C_k(t) = \langle 0|\hat{b}_k\hat{H}_{\mathrm{SB}}(t)\hat{H}_{\mathrm{SB}}(0)\hat{b}^\dagger_k|0\rangle = \frac{1}{4}\sum_a |L_{ka}|^2\,\langle\hat{Q}_a(t)\hat{Q}_a(0)\rangle. \tag{12}$$

We further accept that statistical properties of all sites are the same, then there is a single function $C_k(t) \to C(t)$, which is the most important quantity.

We apply Markovian secular Redfield relaxation theory (MSRT) [15, 16] at the second order with respect to the system–phonon coupling. This coupling leads to the relaxation of excitons. It becomes convenient to denote the Fourier–Laplace transform

$$M(\omega) = \int_0^\infty \exp(\mathrm{i}\omega t)C(t)\,\mathrm{d}t. \tag{13}$$

The real part of this function is responsible for energy relaxation, while the imaginary part is responsible for the bath-induced spectral line shift. It can be also given in terms of the so-called spectral density

$$M(\omega) = \frac{1}{2}\big(1+\coth(\beta\omega/2)\big)C''(\omega) - \mathrm{i}\int\frac{\mathrm{d}\omega'}{2\pi}\frac{1+\coth(\beta\omega'/2)}{\omega'-\omega}C''(\omega'), \tag{14}$$

where $C''(\omega)$ is the temperature independent energy fluctuation spectral density and $\beta = 1/k_{\mathrm{B}}T$, where k_{B} is the Boltzmann constant and T is the temperature. The MSRT approach yields relaxation tensors for all NEE equations.

Exciton–exciton annihilation is yet another relaxation channel. It becomes important at the fifth or higher orders to the optical field. This property has been phenomenologically generalized in Ref. [5] to all NEE variables:

$$\left[\frac{\mathrm{d}A_{nk\ldots}}{\mathrm{d}t}\right)_{\mathrm{EEA}} = -\frac{\kappa_0}{2}\sigma_{mm}\left(G_{mn}+G_{mk}+\ldots\right)A_{nk\ldots}. \tag{15}$$

Here $A_{nk\ldots}$ is an arbitrary NEE variable, and κ_0 is the annihilation parameter. We make a choice of $G_{mn} = (\delta^{(n-n)}_{mn} + \delta_{mn})$. Here $\delta^{(n-n)}_{mn}$ is the nearest neighbours operator, which is 0 for all terms, except when m and n are the nearest neighbours, and δ_{mn} is the regular Kronecker delta function.

The equations are then updated accordingly:

$$\mathrm{i}\frac{\mathrm{d}b_u}{\mathrm{d}t} = \ldots + \mathrm{i}R^{(b)}_{un}b_n - \mathrm{i}\frac{\kappa_0}{2}\sigma_{nn}G_{nu}b_u, \tag{16}$$

$$\mathrm{i}\frac{\mathrm{d}\sigma_{uv}}{\mathrm{d}t} = \ldots + \mathrm{i}R^{(\sigma)}_{uv,mn}\sigma_{mn} - \mathrm{i}\frac{\kappa_0}{2}\sigma_{nn}\left(G_{un}+G_{vn}\right)\sigma_{uv}, \quad (17)$$

$$\mathrm{i}\frac{\mathrm{d}y_{uv}}{\mathrm{d}t} = \ldots + \mathrm{i}R^{(y)}_{uv,mn}y_{mn} - \mathrm{i}\frac{\kappa_0}{2}\sigma_{nn}\left(G_{un}+G_{vn}\right)y_{uv}, \quad (18)$$

$$\mathrm{i}\frac{\mathrm{d}z_{kuv}}{\mathrm{d}t} = \ldots + \mathrm{i}R^{(z)}_{kuv,k'mn}z_{k'mn} - \mathrm{i}\frac{\kappa_0}{2}\sigma_{nn}(G_{kn}+G_{vn})z_{uv}. \quad (19)$$

Here dots '⋯' denote the remaining terms from Eqs. (7–10) (while in the form of expectation values). For the relaxation tensor expressions, we use the tensors from Ref. [5], except for an additional simplification of the triple quantum coherence relaxation tensor (z variable) to $R^{(z)}_{abca'b'c'} = \delta_{bb'}\delta_{cc'}R^{(b)*}_{a} + \delta_{aa'}\delta_{cc'}R^{(b)}_{b} + \delta_{bb'}\delta_{aa'}R^{(b)}_{c}$, while $R^{(y)}_{aba'b'} = \delta_{bb'}R^{(b)}_{a} + \delta_{aa'}R^{(b)}_{b}$ (both in the exciton eigenstate basis) [10]. In the final form, only two tensors, $R^{(b)}_{a,b}$ and $R^{(\sigma)}_{ab,cd'}$ are independent.

2.3. Spectroscopic observables of NEE

Spectroscopic observables are obtained from induced polarization in the material. Taking the expectation value, $P = \langle\hat{P}\rangle$, the induced polarization dynamics in the dipole approximation is given by variable b:

$$\boldsymbol{P}(t) = \boldsymbol{\mu}_m b_m(t) + \text{c.c.} \quad (20)$$

Pump probe spectra are obtained by a two-pulse design, calculated by subtracting the linear first-order components [5]. A more complicated three-pulse design together with phase cycling is used for two-dimensional coherent spectra [11]. Intensity-dependent absorption spectra are supposedly the simplest possible experiment; however, it is usually overlooked. It is the focus of the present study. It can be modelled by simulating the free induction decay process [17]. In this case, the absorption spectra are given by the Fourier transform of the induced polarization after action by the ultrashort optical pulse $\boldsymbol{E}(t) = \boldsymbol{o}\exp(-(\Delta t)^2/2)$, centred at zero time with the Gaussian envelope [1]:

$$S_A(\omega) = \Im m\int_{-\infty}^{+\infty}\mathrm{d}t\exp(\mathrm{i}\omega t)P(t). \quad (21)$$

Vectorial properties of the field in the present study are further dropped by taking all oscillators aligned in one dimension as a linear chain with additional cyclic boundary conditions.

Such calculated absorption spectrum does have excitation intensity dependence since the equations are essentially nonlinear. They will be used to study the variation of the absorption spectrum lineshape as a function of excitation intensity.

3. Closing NEE for numerical calculations

NEE equation factorization is employed to reduce computational costs and to close the hierarchy at a specific selected level. This reduces complexity of calculations but may remove or add new behaviour to spectroscopic results; thus the NEE factorization requires a systematic study, and this is the purpose of the present paper. For example, a simple factorization

$$\langle\hat{b}^\dagger_k\hat{b}^\dagger_n\hat{b}_k\hat{b}_n\hat{b}_n\rangle = \sigma_{kk}z_{nnn} \quad (22)$$

neglects the operator order, and that becomes significant when $k = n$. However, when $k \neq n$, we indeed have an isolated population of the kth chromophore, and the rest are the characteristics of the nth chromophore. In contrast, for other indices, different factorization seems more appropriate:

$$\langle\hat{b}^\dagger_n\hat{b}^\dagger_n\hat{b}_m\hat{b}_m\hat{b}_l\rangle = y^*_{nn}\,y_{mm}\,b_l. \quad (23)$$

Here the operator order is preserved, but another important difference is that the latter description considers all variables as optical coherence terms. It can be expected that the terms related to populations (factorized in the former way) would persist longer compared to the latter factorization into coherences. In these both cases, another effect is neglected when $k = n = m = l$, where the variable $\langle\hat{b}^\dagger_n\hat{b}^\dagger_n\hat{b}_n\hat{b}_n\hat{b}_n\rangle$ is essentially the optical coherence between the 2nd and 3rd molecular excitations. Notice that the variable $\hat{b}_n\hat{b}_n\hat{b}_n$ is the triple excitation coherence and by factorizing the variable we lose associated resonances that could be controlled by paulionicity or bosonicity.

Factorization of high-order variables additionally allows one to avoid deriving relaxation rates for higher-order terms. For the lower-order terms, Redfield relaxation rates are easily expressed in the exciton basis. In the site basis, the terms are cumbersome and quickly become computationally excessive when calculating the higher-order terms.

Below, we present several possible schemes for closing NEE at various levels of complexity.

3.1. Complete factorization

The complete factorization of all variables into the smallest possible $b(t)$ variables allow one to have a very compact form of the equations,

$$\begin{aligned}\mathrm{i}\frac{\mathrm{d}b_u}{\mathrm{d}t} &= \left(1-2\eta b_u^* b_u\right)\left(J_{un}b_n + \left(1-\eta\right)K_u b_u^* b_u^2 + \mu_u^-(t)\right)\\ &+ \mathrm{i}R^b_{un}b_n - \mathrm{i}\frac{\kappa_0}{2}b_m^* b_m G_{mu}b_u. \end{aligned} \tag{24}$$

This equation describes coupled nonlinear oscillators. It is remarkable that the chromophoric anharmonicities are still included as well as the excitation amplitude nonlinearity via the $(1 - 2\eta b_u^* b_u)$ term. However, the double-excitation energy of oscillators is included approximately. Notice that a similar approach has been used to describe highly nonlinear excitations of carbon nanotubes [18].

3.2. Restricted coherent state factorization

If the system remains coherent, the wavefunction description is completely valid, and daggered and non-daggered operators evolve independently. This can be utilized up to double excitations by using only the two equations [5]:

$$\begin{aligned}\mathrm{i}\frac{\mathrm{d}b_u}{\mathrm{d}t} &= J_{un}\left(b_n - 2\eta b_u^* y_{un}\right) + \mu_u^-(t)\left(1-2\eta b_u^* b_u\right)\\ &+ (1-\eta)K_u(b_u^* y_{uu} - 2\eta y_{uu}^* y_{uu} b_u)\\ &+ \mathrm{i}R^b_{un}b_n - \mathrm{i}\frac{\kappa_0}{2}b_m^* G_{mu}y_{mu}, \end{aligned} \tag{25}$$

$$\begin{aligned}\mathrm{i}\frac{\mathrm{d}y_{uv}}{\mathrm{d}t} &= J_{vn}\left(1-2\eta b_v^* b_v\right)y_{un} + J_{un}\left(1-2\eta b_u^* b_u\right)y_{vn}\\ &- 2\eta\delta_{uv}J_{vn}\left(1-2\eta b_v^* b_v\right)y_{vn}\\ &+ \mu_v^-(t)(b_u - 2\eta b_v^* y_{vu}) + \mu_u^-(t)(b_v - 2\eta b_u^* y_{uv})\\ &- 2\delta_{uv}\eta\mu_v^-(t)\left(b_v - 2\eta b_v^* y_{vv}\right)\\ &+ (1-\eta)(K_v b_v^* b_v + K_u b_u^* b_u)\hat{y}_{uv}\\ &+ (1-\eta)\delta_{uv}K_v(1-\eta(3-2\eta)b_v^* b_v)y_{vv}\\ &+ \mathrm{i}R^y_{uvnm}y_{nm}\\ &- \mathrm{i}\frac{\kappa_0}{2}b_m^* b_m G_{mu}y_{uv} - \mathrm{i}\frac{\kappa_0}{2}b_m^* b_m G_{mv}y_{uv}. \end{aligned} \tag{26}$$

Here we have additionally factorized $\langle\hat{b}_v\hat{b}_u\hat{b}_n\rangle = b_v y_{un}$ by breaking triple coherences; the annihilation terms were replaced by changing $\sigma_{nm} = b_n^* b_m$. Notice that the factorization of daggered and undaggered operators holds in the pure state limit when the system is described by a wavefunction; the bra and ket wavefunctions then propagate independently, so daggered and undaggered variables become independent. We call this limit completely coherent. It can be considered only at low temperatures or at short times when the system is in the completely coherent state.

In molecular systems, usually exciton decoherence plays an important role, the system turns into the mixed state, and the coherent model becomes insufficient. σ and z variables include the exciton population variables when bra and ket states become correlated, and thus including these variables in the models is highly desirable when applying the equations to the realistic molecular systems. Therefore, below we study more complex, while more correct approaches.

3.3. Direct factorization

Another alternative is retaining σ and y, using $\hat{g}_v = (1 - 2\eta\hat{\sigma}_{vv})$ as a hint for factorization. Accordingly, first we identify all populations and isolate them. Retaining σ means that we retain population-induced effects that last longer than coherences. This type of factorization should be more suitable for experiments that deal with delay times longer than coherence times. We then obtain the following set of three equations:

$$\begin{aligned}\mathrm{i}\frac{\mathrm{d}b_u}{\mathrm{d}t} &= J_{un}\left(1-2\eta\sigma_{un}\right)b_n + \left(1-\eta\right)K_u\sigma_{uu}b_u\\ &-2\eta(1-\eta)K_u b_u^*\sigma_{uu}y_{uu} + \mu_u^-(t)(1-2\eta\sigma_{uu})\\ &+\mathrm{i}R^{(b)}_{un}b_n - \mathrm{i}\frac{\kappa_0}{2}\sigma_{nn}G_{nu}b_u, \end{aligned} \tag{27}$$

$$\begin{aligned}\mathrm{i}\frac{\mathrm{d}\sigma_{uv}}{\mathrm{d}t} &= J_{vn}\left(\sigma_{un} - 2\eta b_u^*\sigma_{vv}b_n\right)\\ &- J_{mu}\left(\sigma_{mv} - 2\eta b_m^*\sigma_{uu}b_v\right)\\ &+ \mathrm{i}R^{(\sigma)}_{uv,mn}\sigma_{mn} - \mathrm{i}\frac{\kappa_0}{2}\sigma_{nn}(G_{un}+G_{vn})\sigma_{uv}\\ &+ (1-\eta)K_v b_u^*\sigma_{vv}b_v - (1-\eta)K_u b_u^*\sigma_u b_v\\ &+ \mu_v^-(t)b_u^*(1-2\eta\sigma_{vv})\\ &- \mu_u^*(t)(1-2\eta\sigma_{uu})b_v, \end{aligned} \tag{28}$$

$$
\begin{aligned}
&\mathrm{i}\frac{\mathrm{d}y_{uv}}{\mathrm{d}t} = J_{vn}\left(1-2\eta\sigma_{vv}\right)y_{uv} + J_{uv}(1-2\eta\sigma_{uu})y_{vn}\\
&+\mathrm{i}R^{(y)}_{uv,mn}y_{mn} - \mathrm{i}\frac{\kappa_0}{2}\sigma_{nn}(G_{un}+G_{vn})y_{uv}\\
&-2\eta\delta_{uv}J_{vn}(1-2\eta\sigma_{vv})y_{vn}\\
&+\mu_v^-(t)(1-2\eta\sigma_{vv})b_u + \mu_u^-(t)(1-2\eta\sigma_{uu})b_v\\
&-2\delta_{uv}\eta\mu_v^-(t)(1-2\eta\sigma_{vv})b_v\\
&+(1-\eta)(K_v\sigma_{vv}+K_u\sigma_{uu})y_{uv}\\
&+(1-\eta)\delta_{uv}K_v(1-\eta(3-2\eta)\sigma_{vv})y_{vv}.
\end{aligned}
\tag{29}
$$

3.4. Third-order models

The following factorization model keeps at least third-order terms unfactorized and factorizes all higher-order terms in specific schemes. The third order is the lowest nonlinear order process in isotropic samples. Therefore, by keeping at least third-order variables the 'whole' previously known features, we expect, should exist, and then factorization affects only higher-order terms.

All following models rely on the following form of the NEE:

$$
\begin{aligned}
&\mathrm{i}\frac{\mathrm{d}b_u}{\mathrm{d}t} = J_{un}b_n - 2\eta J_{un}z_{uun} + \left(1-\eta\right)K_u z_{uuu}\\
&+\mu_u^-(t) - 2\eta\mu_u^-(t)\sigma_{uu}\\
&+\mathrm{i}R^{(b)}_{un}b_n - \mathrm{i}\frac{\kappa_0}{2}\sigma_{nn}G_{nu}b_u + b_u^{(5)},
\end{aligned}
\tag{30}
$$

$$
\begin{aligned}
&\mathrm{i}\frac{\mathrm{d}\sigma_{uv}}{\mathrm{d}t} = J_{vn}\sigma_{un} - J_{nu}\sigma_{nv} + \mathrm{i}R^{(\sigma)}_{uv,mn}\sigma_{mn}\\
&-\mathrm{i}\frac{\kappa_0}{2}\sigma_{nn}(G_{un}+G_{vn})\sigma_{uv} + \mu_u^-(t)b_u^* - \mu_u^+(t)b_v + \sigma_{uv}^{(4)},
\end{aligned}
\tag{31}
$$

$$
\begin{aligned}
&\mathrm{i}\frac{\mathrm{d}y_{uv}}{\mathrm{d}t} = J_{vn}y_{un} + J_{un}y_{vn} - 2\eta\delta_{uv}J_{vn}y_{vn}\\
&+\mathrm{i}R^{(y)}_{uv,mn}y_{mn} - \mathrm{i}\frac{\kappa_0}{2}\sigma_{nn}(G_{un}+G_{vn})y_{uv}\\
&+(1-\eta)\delta_{uv}K_v y_{vv} + \mu_v^-(t)b_u + \mu_u^-(t)b_v\\
&-2\eta\delta_{uv}\mu_v^-(t)b_v + y_{uv}^{(4)},
\end{aligned}
\tag{32}
$$

$$
\begin{aligned}
&\mathrm{i}\frac{\mathrm{d}z_{kuv}}{\mathrm{d}t} = J_{vn}z_{kun} + J_{un}z_{kvn} - 2\eta\delta_{uv}J_{vn}z_{kvn}\\
&+\mathrm{i}R^{(z)}_{kuv,k'mn}z_{k'mn} - \mathrm{i}\frac{\kappa_0}{2}\sigma_{nn}(G_{kn}+G_{un}+G_{vn})z_{kuv}\\
&-J_{mk}z_{muv} + (1-\eta)\delta_{uv}K_v z_{kvv}\\
&+\mu_v^-(t)\sigma_{ku} + \mu_u^-(t)\sigma_{kv} - 2\eta\delta_{uv}\mu_v^-(t)\sigma_{kv}\\
&+\mu_k^*(t)y_{uv} + 2\eta\mu_k^*(t)z_{kuv}b_k + z_{kuv}^{(5)}.
\end{aligned}
\tag{33}
$$

Here $b^{(5)}$ and $z^{(5)}$ are the fifth-order corrections, while $y^{(4)}$ and $\sigma^{(4)}$ are the fourth-order corrections.

In the present case, the main downside compared to simpler models is that we keep $R^z_{kmn,luv}$ terms, which come from the Redfield relaxation theory. Annihilation terms are kept the same for all models.

3.4.1. zσ factorization model

In the next factorization model, which we denote by the $z\sigma$-based factorization, we factorize all terms higher than the third order in terms of σ and lower-order variables. From the set of above-given NEE we end up with high-order corrections

$$
b_u^{(5)} = -2\eta(1-\eta)K_u\sigma_{uu}z_{uuu},
\tag{34}
$$

$$
\begin{aligned}
&\sigma_{uv}^{(4)} = -2\eta J_{vn}\sigma_{vv}\sigma_{un} - 2\eta J_{nu}\sigma_{uu}\sigma_{nv}\\
&+(1-\eta)\left(K_v\sigma_{vv} - K_u\sigma_{uu}\right)\sigma_{uv}\\
&-2\eta\mu_v^-(t)z^*_{uvv} + 2\eta\mu_u^+(t)z_{uuv},
\end{aligned}
\tag{35}
$$

$$
\begin{aligned}
&y_{uv}^{(4)} = -2\eta J_{un}\sigma_{uu}y_{vn} - 2\eta J_{vn}\sigma_{vv}y_{un}\\
&+(1-\eta)\left(K_v\sigma_{vv} + K_u\sigma_{uu}\right)y_{uv}\\
&-\eta(2\eta-3)(\eta-1)\delta_{uv}K_v\sigma_{vv}y_{vv}\\
&-2\eta\mu_u^-(t)z_{uuv} - 2\eta\mu_v^-(t)z_{vvu}\\
&+4\eta^2\delta_{uv}J_{vn}\sigma_{vv}y_{vn} + 4\eta^2\delta_{uv}\mu_v^-(t)z_{vvv},
\end{aligned}
\tag{36}
$$

$$
\begin{aligned}
&z_{kuv}^{(5)} = 2\eta J_{mk}\sigma_{kk}z_{muv} - 2\eta J_{un}\sigma_{uu}z_{kvn}\\
&-2\eta J_{vn}\sigma_{vv}z_{kun} + 2\eta\mu_k^+(t)\sigma_{kk}y_{uv}\\
&+(1-\eta)\left(K_v\sigma_{vv} + K_u\sigma_{uu} - K_k\sigma_{kk}\right)z_{kuv}\\
&-\eta(2\eta-3)(\eta-1)\delta_{uv}K_v\sigma_{vv}z_{kvv}\\
&-2\eta\mu_u^-(t)\sigma_{uu}\sigma_{kv} - 2\eta\mu_v^-(t)\sigma_{vv}\sigma_{ku}\\
&+4\eta^2\delta_{uv}J_{vn}\sigma_{vv}z_{kvn} + 4\eta^2\delta_{uv}\mu_v^-(t)\sigma_{vv}\sigma_{kv}.
\end{aligned}
\tag{37}
$$

The terms like $\langle\hat{b}_u^\dagger\hat{b}_i^\dagger\hat{b}_v\hat{b}_n\rangle$ are factorized like $\sigma_{vv}\sigma_{un}$, and we take the assumption that $\langle\hat{b}_v^\dagger\hat{b}_v\rangle$ is population and it quickly loses coherence with other terms.

3.4.2. zz factorization model

Alternatively, we factorize all terms higher than the third order in terms of z and lower-order terms. Compared to the $z\sigma$ factorization scheme, the operator order in zz factorization is preserved. We expect to see a difference from $z\sigma$ as we preserve more double coherence terms, as these all are split apart:

$$b_u^{(5)} = -2\eta(1-\eta)K_u z^*_{uuu} y_{uu}, \tag{38}$$

$$\begin{aligned}\sigma_{uv}^{(4)} &= -2\eta J_{vn} z^*_{uvv} b_n + 2\eta J_{mu} b^*_m z_{uuv} \\ &+ (1-\eta)K_v b^*_u z_{vvv} - (1-\eta)K_u z^*_{uuu} b_v \\ &- 2\eta\mu_v^-(t) z^*_{uvv} + 2\eta\mu_u^+(t) z_{uuv},\end{aligned} \tag{39}$$

$$\begin{aligned}y_{uv}^{(4)} &= -2\eta J_{un} z_{uuv} b_n - 2\eta J_{vn} z_{vuv} b_n \\ &- \eta(2\eta-3)(\eta-1)\delta_{uv} K_v z_{vvv} b_v \\ &(1-\eta)K_v z_{vvv} b_u + (1-\eta)K_u z_{uuu} b_v \\ &- 2\eta\mu_u^-(t) z_{uuv} - 2\eta\mu_v^-(t) z_{vvu} \\ &+ 4\eta^2\delta_{uv} J_{vn} z_{vvv} b_n + 4\eta^2\delta_{uv}\mu_v^-(t) z_{vvv},\end{aligned} \tag{40}$$

$$\begin{aligned}z_{kuv}^{(5)} &= 2\eta J_{mk} z^*_{mkk} y_{uv} - 2\eta J_{un} z^*_{kuu} y_{vn} \\ &- 2\eta J_{vn} z^*_{kvv} y_{un} - (1-\eta)K_k z^*_{kkk} y_{uv} \\ &- 2\eta\mu_u^-(t) b^*_k z_{uuv} - 2\eta\mu_v^-(t) b^*_k z_{vuv} \\ &+ (1-\eta)\left(K_v z^*_{kuu} + K_u z^*{}_{kuu}\right) y_{uv} \\ &+ 4\eta^2\delta_{uv} J_{vn} z^*_{kvv} y_{vn} + 4\eta^2\delta_{uv}\mu_v^-(t) b^*_k z_{vvv} \\ &- \eta(2\eta-3)(\eta-1)\delta_{uv} K_v z^*_{kvv} y_{vv}.\end{aligned} \tag{41}$$

3.4.3. zn factorization

Noting the 'natural' structure that comes from the commutation relation $\hat{g}_u = (1 - 2\eta\hat{\sigma}_{uu})$, we can attempt to keep the σ_{uu} and preserve the order of operators, for example: $\langle \hat{b}_u b_u^\dagger \hat{b}_u \hat{b}_u^\dagger \hat{b}_u^\dagger \rangle \to b^*_u \sigma_{uu} y_{uu}$. This factorization scheme should give similar results to the zz scheme; however, its credibility can be inspected separately:

$$b_u^{(5)} = -2\eta(1-\eta)K_u b^*_u \sigma_{uu} y_{uu}, \tag{42}$$

$$\begin{aligned}\sigma_{uv}^{(4)} &= -2\eta J_{vn} b^*_u \sigma_{vv} b_n - 2\eta J_{nu} b^*_n \sigma_{uu} b_v \\ &+ (1-\eta)K_v b^*_u - 2\eta\mu_v^-(t) z^*_{vvu} + 2\eta\mu_u^+(t) z_{uuv},\end{aligned} \tag{43}$$

$$\begin{aligned}y_{uv}^{(4)} &= -2\eta J_{vn}\sigma_{vv} y_{un} - 2\eta J_{un}\sigma_{uu} y_{vn} \\ &- (1-\eta)\eta(3-2\eta)\delta_{uv} K_v \sigma_{vv} y_{vv} \\ &+ (1-\eta)\left(K_v\sigma_{vv} + K_u\sigma_{uu}\right) y_{uv} \\ &- 2\eta\mu_v^-(t) z_{vvu} - 2\eta\mu_u^-(t) z_{uuv} \\ &+ 4\eta^2\delta_{uv} J_{vn}\sigma_{vv} y_{vn} + 4\eta^2\delta_{uv}\mu_v^-(t) z_{vvv},\end{aligned} \tag{44}$$

$$\begin{aligned}z_{kuv}^{(5)} &= -2\eta J_{vn} b^*_k \sigma_{vv} y_{un} - 2\eta J_{un} b^*_k \sigma_{uu} y_{vn} \\ &+ 2\eta J_{mk} b^*_m \sigma_{kk} y_{uv} + 2\eta\mu_k^+(t)\sigma_{kk} y_{uv} \\ &- 2\eta\mu_v^-(t) b^*_k \sigma_{vv} b_u - 2\eta\mu_u^-(t) b^*_k \sigma_{uu} b_v \\ &+ 4\eta^2\delta_{uv} J_{vn} b^*_k \sigma_{vv} y_{vn} + 4\eta^2\delta_{uv}\mu_v^-(t) b^*_k \sigma_{vv} b_v \\ &+ (1-\eta) b^*_k \left(K_v\sigma_{vv} + K_u\sigma_{uu} - K_k\sigma_{kk}\right) y_{uv} \\ &- (1-\eta)\eta(3-2\eta)\delta_{uv} K_v b^*_k \sigma_{vv} y_{vv}.\end{aligned} \tag{45}$$

4. Model system

Different levels of theory will be tested on the model system, which is a linear J aggregate of seven chromophores. This is a simple linear chain of chromophores, which shows superradiant absorption, red-shifted from the independent chromophore [19]. Parameters of the model are taken from typical tubular J aggregates [20, 21]. The nearest-neighbour resonant coupling $J_{nn+1} = J_{n+1n} = -800$ cm^{-1} and ends are connected with periodic boundary conditions. Periodic conditions represent an infinitely long linear aggregate. Additionally, we include the diagonal Gaussian energy disorder of $\sigma = 100$ cm^{-1} to perturb the ideal symmetry of the aggregate. The excitation energy J_{nn} of all sites is set at 18000 cm^{-1}. On-site energy anharmonicity (only needed when $\eta \neq 1$) is taken as $K_{nn} = +1000$ cm^{-1}. For the quantum particle statistics, we include 3 different cases: bosons $\eta = 0$, paulions $\eta = 1$ and the intermediate regime, $\eta = 0.5$.

For system–phonon interaction we use the Drude spectral density

$$C''(\omega) = 2\lambda \frac{\omega\Lambda}{\omega^2 + \Lambda^2}, \tag{46}$$

with $\lambda = 20$ cm^{-1} and $\Lambda = 50$ cm^{-1}. The system temperature $T = 300$ K. For the annihilation parameter we set $\kappa_0 = 1000$ cm^{-1}.

As we include EEA terms, the optical excitation field intensity becomes an important parameter. The optical field envelope is defined as $E(t) = AE_0(t)$, $A7$is the amplitude, and $E_0(t)$ is the normalized envelope function

$$E_0(t) = \frac{1}{s\sqrt{2\pi}} \exp\left(-\frac{t^2}{2s^2}\right), \tag{47}$$

$$s = \frac{2\sqrt{2}}{\Delta\omega_{\mathrm{FWHM}}\sqrt{\ln 2}}. \tag{48}$$

The molecule transition dipole moments are taken such that

$$s = \frac{2\sqrt{2}}{\Delta\omega_{\mathrm{FWHM}}\sqrt{\ln 2}}, \tag{49}$$

where A_0 is the excitation with the external optical field scaling constant. The factor of $\sqrt{7}$ is included by keeping in mind that when transforming such a system into the exciton basis, the lowest exciton has a transition dipole moment scaled as $\sqrt{N}$, where N is the number of molecules in such a system. This way allows one to relate A_0 to population in the lowest energy exciton approximately as $\sigma \sim A_0^2$ ignoring any saturation effects, delocalization, etc.

5. Results

First, we present the results without EEA. Starting with the 3 simplest models – a coherent model (Eqs. (25, 26)) marked as **coh**, a direct factorization (Eqs. (27–29)) marked as ***s***, and a third-order pure unfactorized model (Eqs. (30–33)) marked as ***z*3** – we present the comparison of these models with no EEA in Fig. 1. Here, we show the intensity-dependent absorption spectra. We see a wildly different behaviour between these models when the field intensity is increased. For a coherent model, a second peak appears and grows with the field intensity. This additional peak can be associated with induced excited state absorption (ESA) appearing from the already excited main exciton band into the higher levels. This ESA peak grows weakly compared to other models, as coherences are short lived so higher-order terms are more suppressed with this factorization. In contrast, the *s* model, which preserves populations, shows no extra peak, only the whole main absorption line shifts to higher energy. In addition, we observe a change in the lineshape, the peak appears to be 'tilted' to the blue, the blue side gets steeper with intensity, while the red side gets shallower. The third-order model ***z*3** has a similar behaviour as the coh model, except the side peak is much narrower, consequently, has a much larger amplitude. Notably, the excitation intensity effects are much more pronounced for paulions, which is a much more complicated nonlinear system.

Next, we compare models, where factorization is performed at fourth-order terms (the terms higher than the third order are factorized); the models are labelled as ***zσ*4**, which corresponds to Eqs. (35, 36), ***zz*4** corresponds to Eqs. (39, 40), and ***zn*4** corresponds to Eqs. (43, 44), where these terms are added to ***z*3** terms. We present the intensity dependent spectra of these models in Fig. 2. What we find is that all three models show a similar behaviour as the ***z*3** model, consequently, the contribution from factorization at fourth-order terms is small. The main reason for this is likely because the fourth order does not 'directly' contribute to polarization, where the third order is dominating, i.e. ***z*** in *b* and the fifth order inside ***z***. Even order terms appear mostly responsible for scaling of the transition dipole moment, which is again a small contribution.

The factorization can be performed at fifth-order contributions. Then, we label models as the ***zσ*5** model (Eqs. (34, 37)), ***zz*5** model (Eqs. (38, 41)) and ***zn*5** model (Eqs. (42, 45)). We see a wildly differing behaviour between factorization schemes (Fig. 3); however, the common feature is again related to the appearance of a separate ESA peak, which grows with increasing field intensity. In the present case, the ESA amplitude is again much weaker than in Fig. 2. It can be observed that some features of low-order factorization models reappear in these models: for the *zz*5 model, which is the population favouring model, we see that the ESA peak shifts to higher energy when field intensity increases, partially mirroring the *s* model, where the whole absorption was shifted. The ***zz*5** model shows a stranger

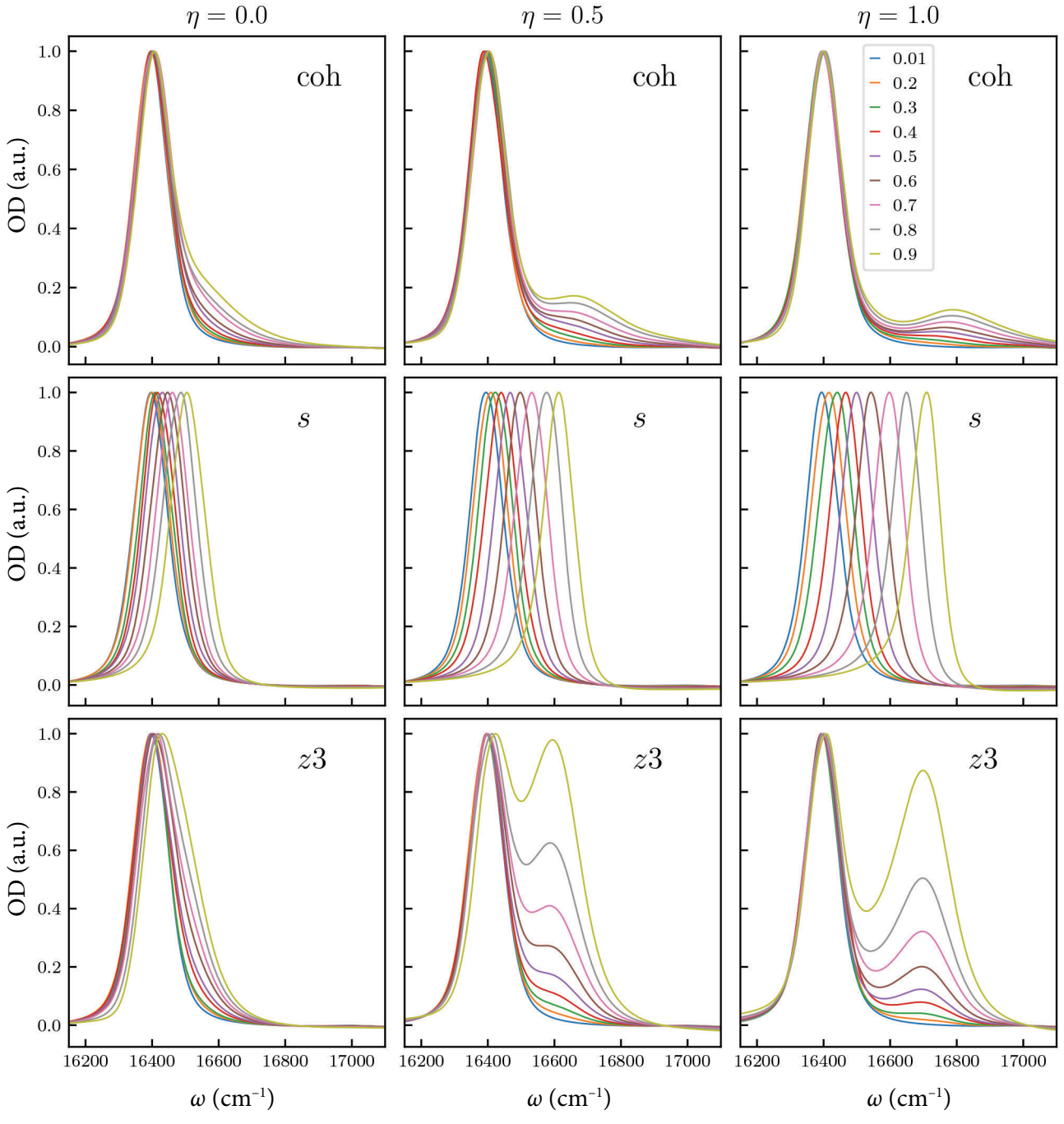

Fig. 1. Absorption of J aggregate for different factorization models (coh, *s* and *z*3) at different excitation optical field intensity values, without EEA.

behaviour. It is the only case where we see negative regions in spectra. These features should be interpreted as the induced emission contribution. The *zn*5 model appears most consistent as it shows a similar behaviour to *zσ*4, *zn*4 and *z*3 models.

Next, we look at the same models with the EEA process included. Looking at the simpler models first (Fig. 4), we see that EEA leads to an excessive broadening of ESA features. Still, the *s* model is the only model demonstrating a shift of the whole absorption band with field intensity. An additional small dip for high-excitation intensities on the red side for the paulion case implies the presence of induced emission as in the *zz*5 model in Fig. 3. ESA in the coherent model has a significantly lower ESA intensity. The absorption spectra for the model *z*3 with EEA terms are broadened, with a significant shoulder reflecting ESA.

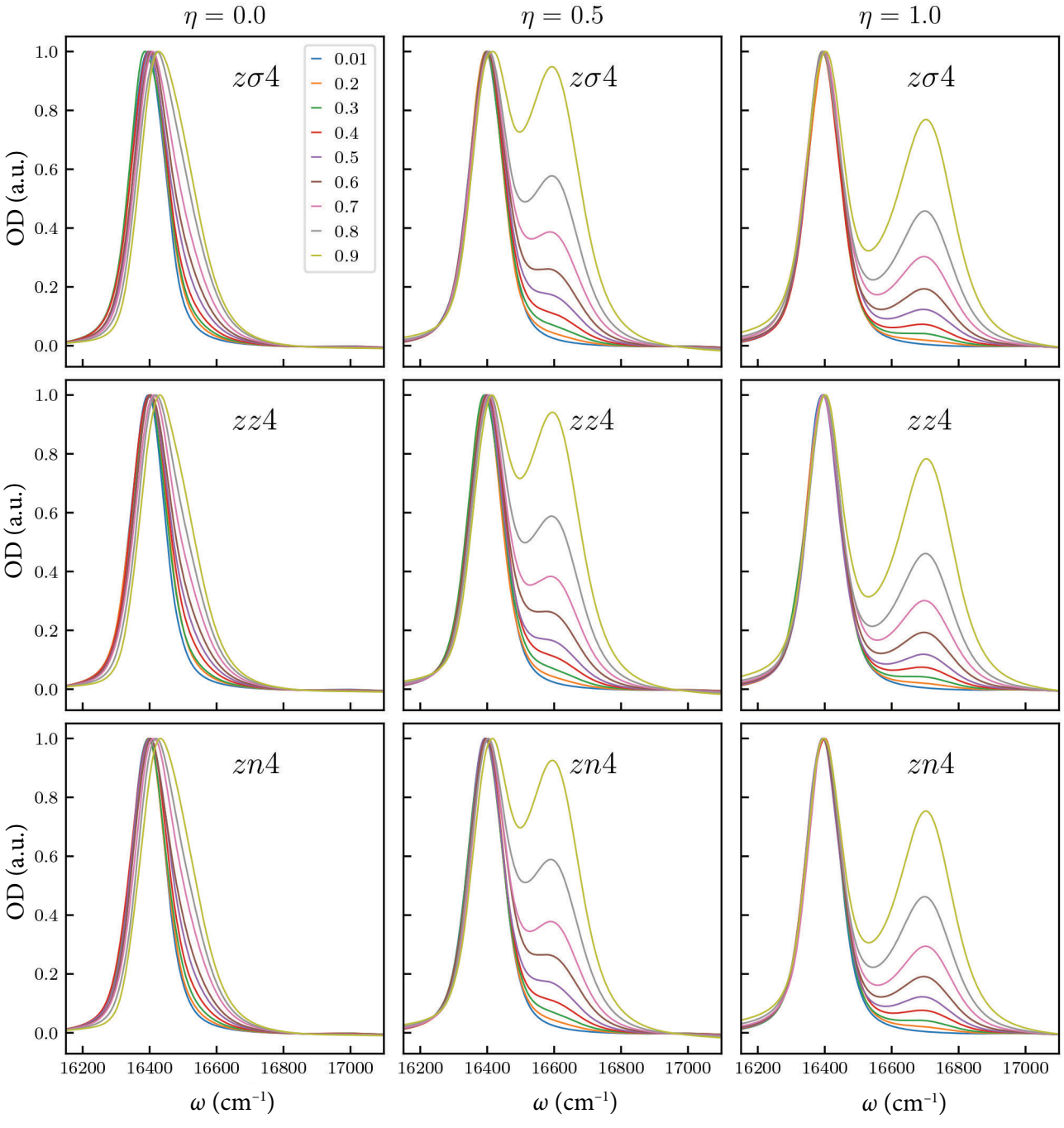

Fig. 2. Absorption of J aggregate for different factorization models (z with fourth-order factorized terms models) at different excitation optical field intensity values, without EEA.

Fourth-order factorized models (Fig. 5) are similarly affected by EEA, mimicking the $z3$ model. Surprisingly, the differences between different factorizations become very small.

With EEA, the fifth-order models (Fig. 6) again differ much less between themselves and from the fourth-order models. Apparently, the large broadening induced by EEA hides differences between the fourth- and fifth-order factorization models.

6. Discussion

Various factorizations of NEE equations are associated with different models of optical response, enhancing specific phenomena. High-order terms (which were factorized) come from specific types of nonlinearities in the system. The target of the research is to identify specific important phenomena and then to associate them with

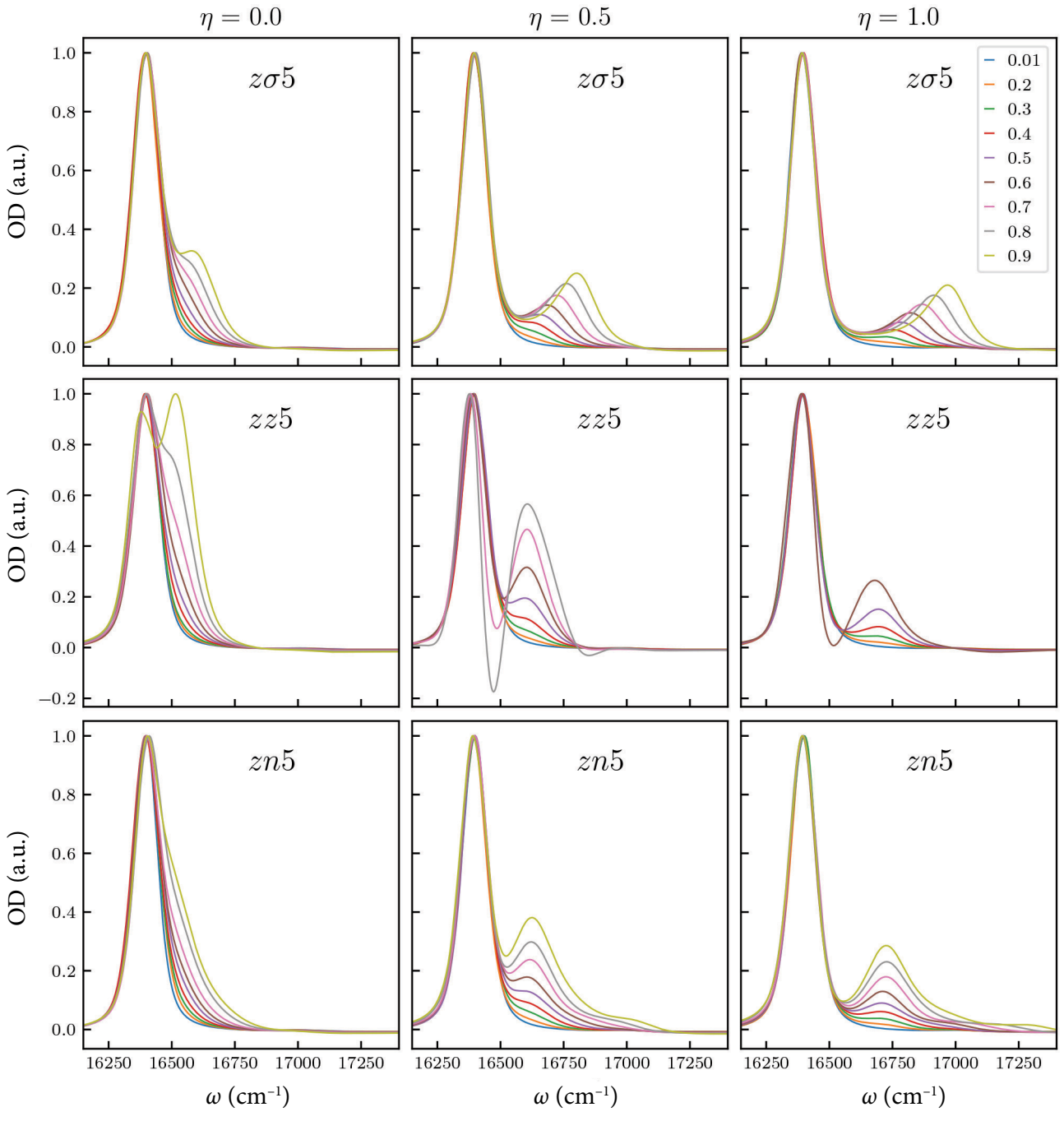

Fig. 3. Absorption of J aggregate for different factorization models (z with fifth-order factorized terms models) at different excitation optical field intensity values, without EEA.

specific variables, so that specific processes can be pointed out when analyzing corresponding experiments.

First of all, it should be noted that at low intensities all models yield the same absorption spectra (even independent of η value). We show this in Fig. 7, where all the absorptions overlap, with negligible differences that come from the finite static disorder averaging.

This can also be observed from the equations, where in all models dropping out nonlinear terms (vanishing at low intensity) we find the simple linear model defined by a single equation

$$\mathrm{i}\frac{\mathrm{d}b_u}{\mathrm{d}t} = J_{un}b_n + \mu_u^{-}(t) + \mathrm{i}R_{un}^{(b)}b_n. \tag{50}$$

This equation is equivalent to the linear response theory. Polarization becomes directly related to

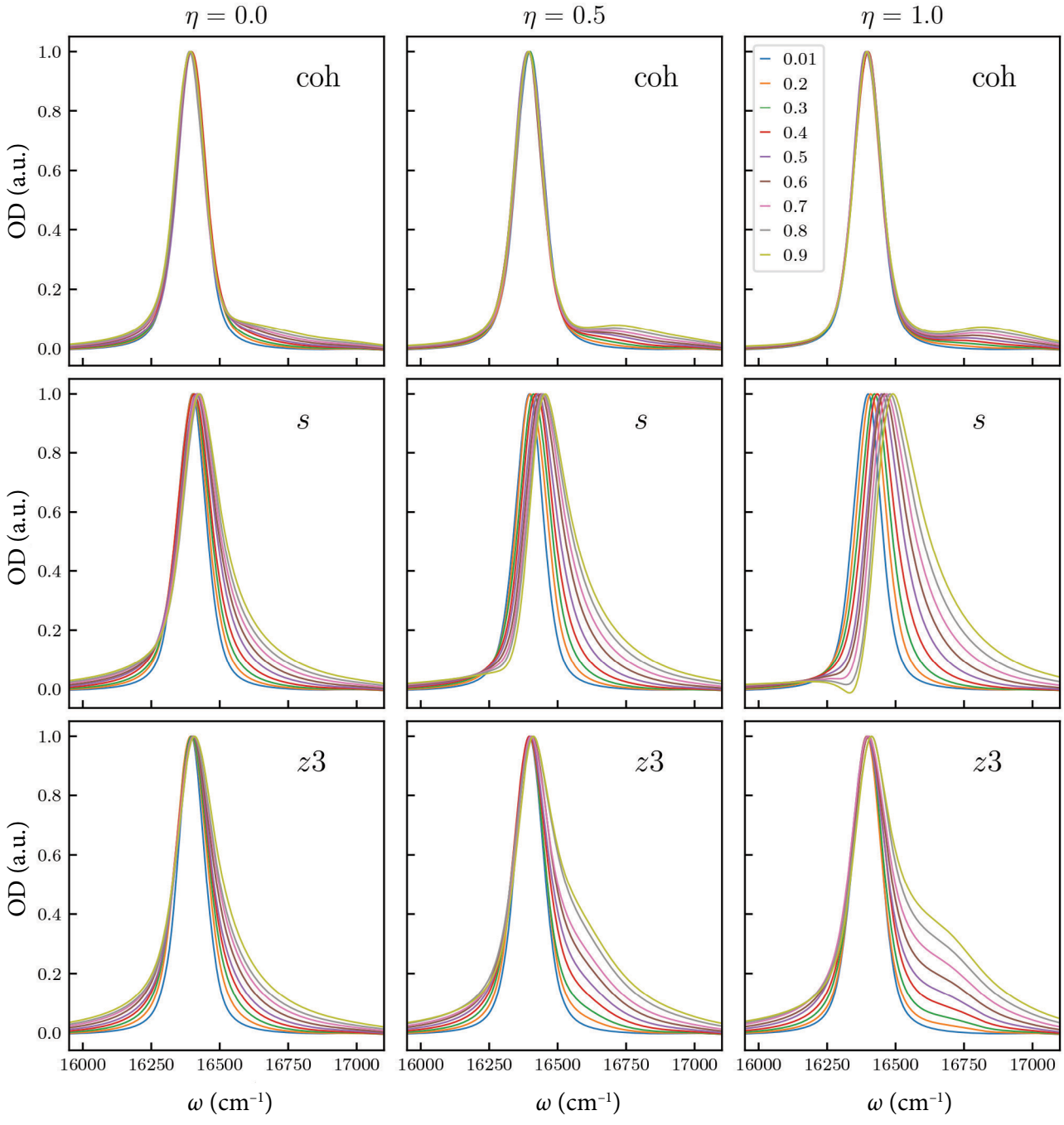

Fig. 4. Absorption of J aggregate for different factorization models (coh, s and $z3$) at different excitation optical field intensity values, with EEA.

the $\hat{b}(t)$ time dependence, which can be solved analytically in the exciton eigenstate representation. The solution then yields the single excitonic Lorentzian peak observed in Fig. 7.

At higher field intensity, nonlinear terms become contributing ones and can be employed in efficient analysis [22]. We observe that most nonlinear nontrivial contributions come from odd-order terms. Polarization is directly related to $\hat{b}(t)$, which relates to $\hat{b}^\dagger\hat{b}\hat{b}$, related to $\hat{b}^\dagger\hat{b}^\dagger\hat{b}\hat{b}\hat{b}$, which relates to seventh-order similar terms, and this continues *ad infinitum*. In our case, we limit ourselves to third- and fifth-order operator configurations as the EEA does not allow for the creation of very high excitation levels. We find that going from the third to the fourth order the change is minimal (only intensity is affected). But going to the fifth order, additional changes become significant:

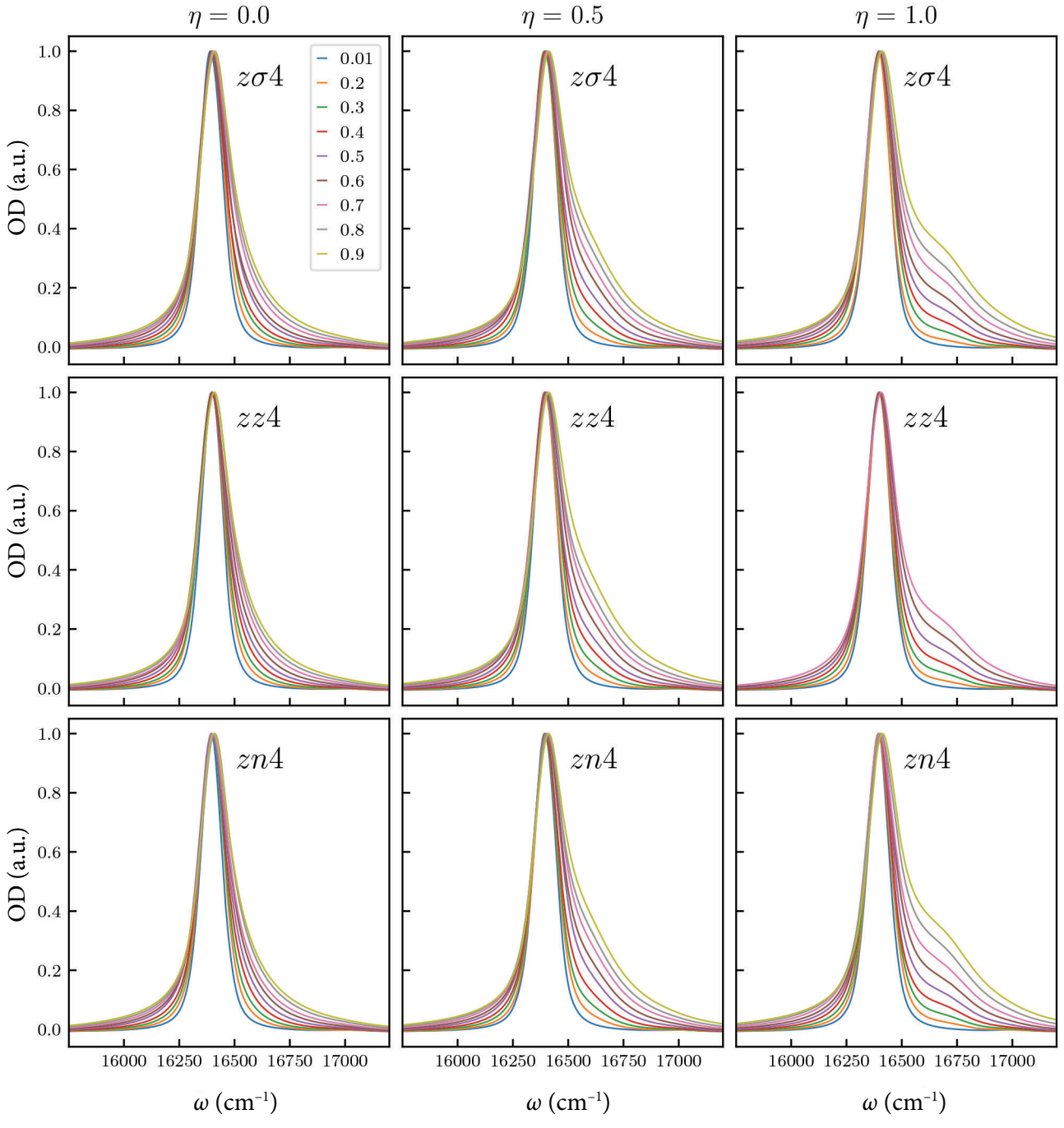

Fig. 5. Absorption of J aggregate for different factorization models (z with fourth-order factorized terms models) at different excitation optical field intensity values, with EEA.

ESA intensity drops to 1/3 of its intensity in third- and fourth-order cases.

Small but significant differences between different types of factorizations can be observed. In cases which favour populations in factorization and disregard the operator order, the ESA peak position becomes dependent on excitation intensity, while when applying more rigid factorization with preserving the operator order, the ESA peak position is stable over excitation intensities.

Curiously, when factorizing in bigger blocks (factorizing with third-order terms instead of second-order ones), we see some instability and even negative amplitudes in 'absorption' spectra. These negative features are related to the type of the 'measurement' that we consider. Note that, in general, we analyze

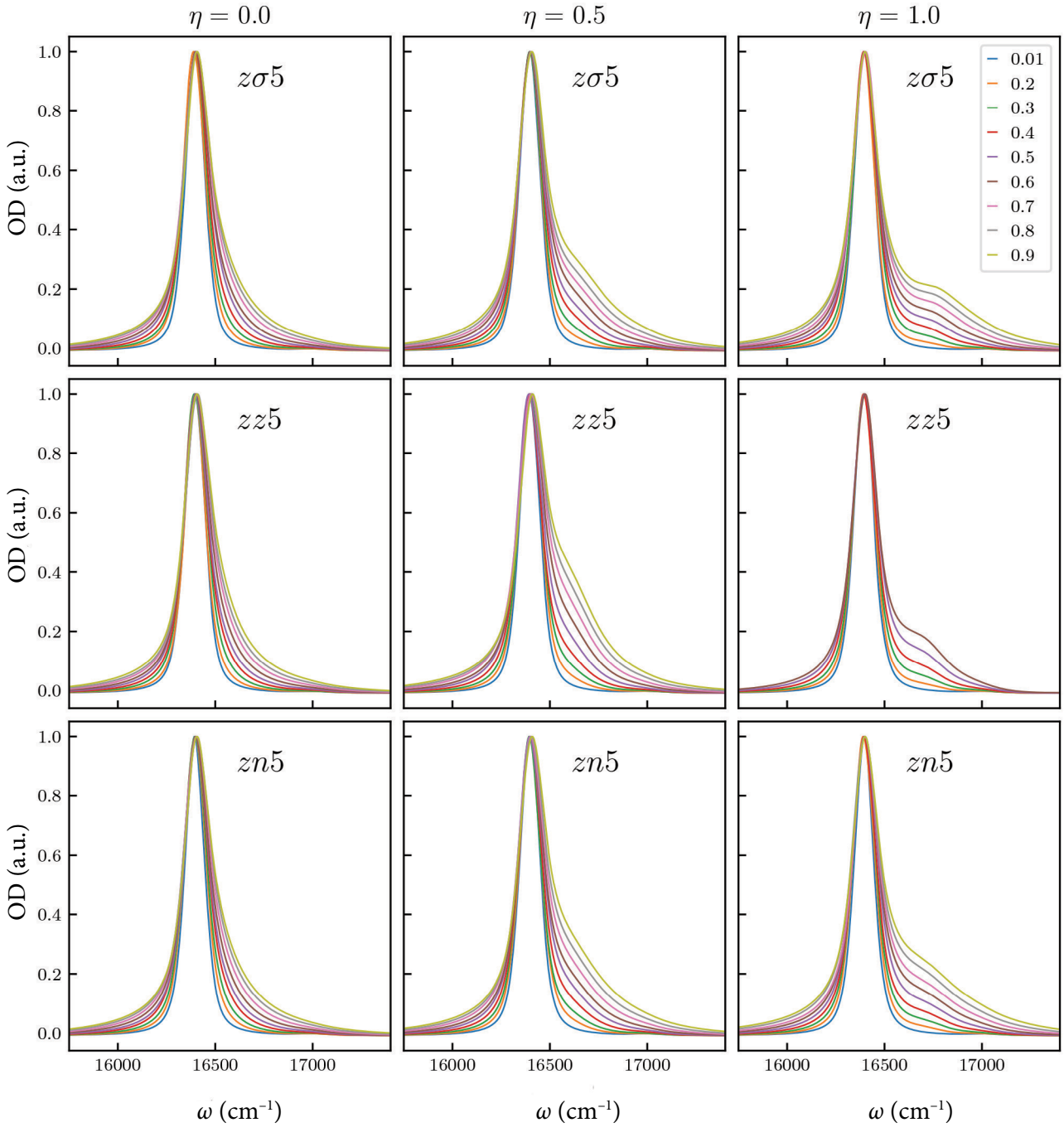

Fig. 6. Absorption of J aggregate for different factorization models (z with fifth-order factorized terms models) at different excitation optical field intensity values, with EEA.

the Fourier transformation of polarization decay after a short excitation. As a result, both the induced absorption and stimulated emission have to be considered. The emission leads to negative features. Different spectra should be obtained by simulating a high-intensity CW measurement. In that case, at strong excitation intensities, we should observe additional peak shifts coming from polaritonic effects.

As already noted, the main reason why the factorization is included is to close the hierarchy of equations due to limited computational resources. The mathematically exact approach is given by the infinite hierarchy of equations, which cannot be implemented in calculations. However, the 'best' factorization method does not exist – different factorization approaches enhance

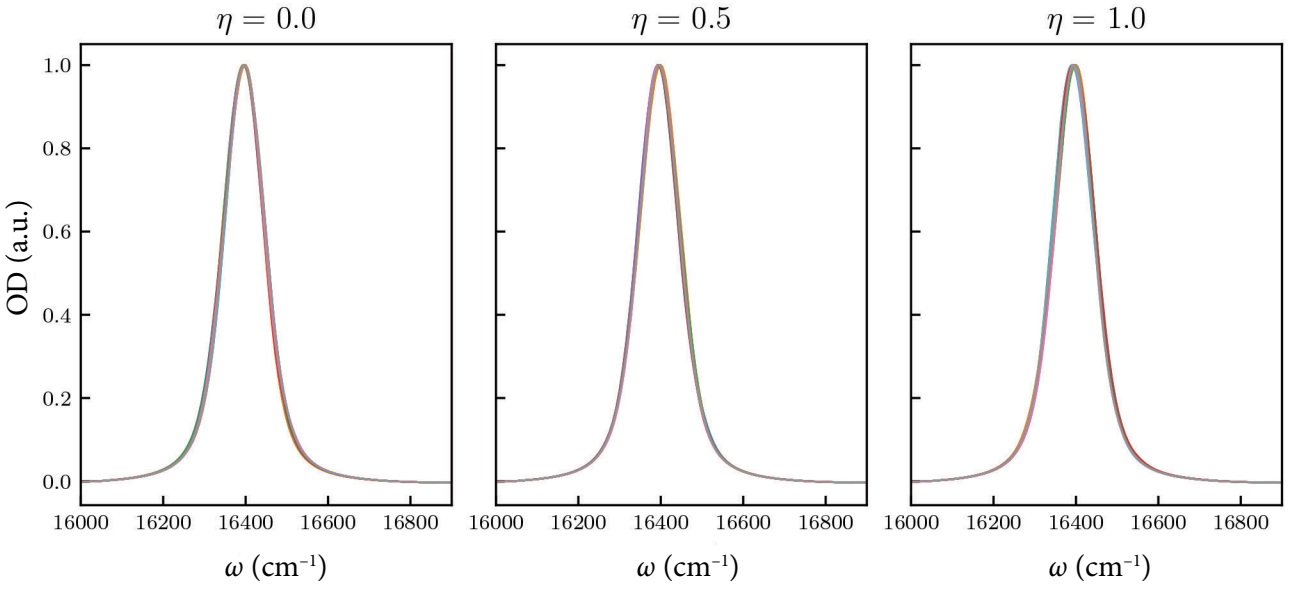

Fig. 7. The absorption of all models presented for both no and with annihilation at low intensity.

different phenomena and should be chosen when considering specific experiments. For example, if only the shift of absorption line with excitation intensity is observed, the *s* model, one of the simplest models, can be used. If the separate excited state absorption is observed, including *z* variable may be important.

Different types of factorization lead to a distinct simplification of equations which lead to efficient and fast computations. The simplest set of equations certainly lead to very fast calculations. Alternatively, some other types lead to instabilities: note that the *zz*5 model even fails to converge for high-intensity cases. The reason why we see instability could be related to the fact that with lower-order terms the commutation-induced symmetry is preserved, while factorizations may break this symmetry, for example, if we have $\langle \hat{b}^\dagger \hat{b}^\dagger \hat{b}\hat{b} \rangle \rightarrow \langle \hat{b}^\dagger \hat{b} \rangle \langle \hat{b}^\dagger \hat{b} \rangle$, both $\hat{b}\hat{b}$ and $\hat{b}^\dagger \hat{b}^\dagger$ get broken and double-excitation characteristics implied by commutation relations are disregarded; but if we have $\langle \hat{b}^\dagger \hat{b}^\dagger \hat{b}\hat{b} \rangle \rightarrow \langle \hat{b}^\dagger \hat{b}^\dagger \hat{b} \rangle \langle \hat{b} \rangle$, the breaking is introduced only partially and the imbalance between various terms could be introduced, which may lead to diverging solutions.

Differences between different equation models become smoothed out by including EEA. Coherent and direct factorization schemes stand out and show more significant differences from others. While the spectra become much more similar with EEA, instability from the *zn* model at high intensity remains. But the instability becomes apparent for larger intensities compared to the case with no annihilation.

Concluding, we show that absorption spectra of molecular systems can be enhanced by additional features at high-excitation intensities. This can be addressed using the non-perturbative propagation of NEE. The equations have to be closed for numerical implementation and there are numerous ways to close the equations. The most interesting approach relies on the factorization of various highly nonlinear terms in NEE. Different types of factorizations may enhance various processes, and this can be utilized in specific applications of NEE. The whole analysis becomes even less complicated when including EEA, because EEA does not allow for the creation of highly excited states. Therefore, EEA diminishes differences between different schemes of factorization. As a result, the NEE application to the systems with EEA is efficient and the calculations can rely on simple equations.

Acknowledgements

We thank the Research Council of Lithuania for financial support (Grant No. S-MIP-23-48). Computations were performed on resources at the High Performance Computing Center, HPC Saulėtekis, of the Faculty of Physics, Vilnius University.

References

[1] S. Mukamel, *Principles of Nonlinear Optical Spectroscopy* (Oxford University Press, New York, 1995).

[2] B. Brüggemann and T. Pullerits, Nonperturbative modeling of fifth-order coherent multidimensional spectroscopy in light harvesting antennas, New J. Phys. **13**, 025024 (2011).

[3] V. Barzda, V. Gulbinas, R. Kananavicius, V. Cervinskas, H. van Amerongen, R. van Grondelle, and L. Valkunas, Singlet–singlet annihilation kinetics in aggregates and trimers of LHCII, Biophys. J. **80**, 2409 (2001).

[4] V. May, Kinetic theory of exciton–exciton annihilation, J. Chem. Phys. **140**, 054103 (2014).

[5] V. Bubilaitis, J. Hauer, and D. Abramavicius, Simulations of pump probe spectra of a molecular complex at high excitation intensity, Chem. Phys. **527**, 110458 (2019).

[6] C.J. Bardeen, The structure and dynamics of molecular excitons, Annu. Rev. Phys. Chem. **65**, 127 (2014).

[7] J. Süß, J. Wehner, J. Dostál, T. Brixner, and V. Engel, Mapping of exciton–exciton annihilation in a molecular dimer via fifth-order femtosecond two-dimensional spectroscopy, J. Chem. Phys. **150**, 104304 (2019).

[8] V. Chernyak, W.M. Zhang, and S. Mukamel, Multidimensional femtosecond spectroscopies of molecular aggregates and semiconductor nanostructures: The nonlinear exciton equations, J. Chem. Phys. **109**, 9587 (1998).

[9] V. Chernyak and S. Mukamel, Third-order optical response of intermediate excitons with fractional nonlinear statistics, J. Opt. Soc. Am. B **13**, 1302 (1996).

[10] V. Bubilaitis and D. Abramavicius, Compact modeling of highly excited linear aggregates using generalized quantum particles, Chem. Phys. **588**, 112445 (2025).

[11] V. Bubilaitis and D. Abramavicius, Signatures of exciton–exciton annihilation in 2DES spectra including up to six-wave mixing processes, J. Chem. Phys. **161**, 104106 (2024).

[12] V. Agranovich and B. Toshich, Collective properties of Frenkel excitons, Sov. Phys. JETP **26**, 104 (1968).

[13] V.M. Agranovich, *Excitations in Organic Solids*, ed. G. Czajkowski, International Series of Monographs on Physics, Ser. No. v.142 (Oxford University Press Inc., Oxford, 2009).

[14] D. Abramavicius, B. Palmieri, D.V. Voronine, F. Šanda, and S. Mukamel, Coherent multidimensional optical spectroscopy of excitons in molecular aggregates; quasiparticle versus supermolecule perspectives, Chem. Rev. **109**, 2350 (2009).

[15] L. Valkunas, D. Abramavicius, and T. Mančal, *Molecular Excitation Dynamics and Relaxation* (Wiley-VCH Verlag GmbH & Co. KGaA, Weinheim, Germany, 2013).

[16] A.G. Redfield, On the theory of relaxation processes, IBM J. Res. Dev. **1**, 19 (1957).

[17] I. Coddington, W.C. Swann, and N.R. Newbury, Time-domain spectroscopy of molecular free-induction decay in the infrared, Opt. Lett. **35**, 1395 (2010).

[18] D. Abramavicius, Y.-Z. Ma, M.W. Graham, L. Valkunas, and G.R. Fleming, Dephasing in semiconducting single-walled carbon nanotubes induced by exciton-exciton annihilation, Phys. Rev. B 79, 195445 (2009).

[19] T. Kobayashi, ed., *J-aggregates* (World Scientific, Singapore, 2012).

[20] B. Kriete, J. Lüttig, T. Kunsel, P. Malý, T.L.C. Jansen, J. Knoester, T. Brixner, and M.S. Pshenichnikov, Interplay between structural hierarchy and exciton diffusion in artificial light harvesting, Nat. Commun. **10**, 4615 (2019).

[21] F. Milota, V.I. Prokhorenko, T. Mancal, H. von Berlepsch, O. Bixner, H.F. Kauffmann, and J. Hauer, Vibronic and vibrational coherences in two-dimensional electronic spectra of supramolecular J-aggregates, J. Phys. Chem. A 117, 6007 (2013).

[22] J. Lüttig, S. Mueller, P. Malý, J. J. Krich, and T. Brixner, Higher-order multidimensional and pump–probe spectroscopies, J. Phys. Chem. Lett. **14**(33), 7556–7573 (2023).

NETIESINIŲ EKSITONŲ LYGČIŲ FAKTORIZAVIMAS: NEARTUTINIS SUGERTIES SPEKTRŲ MODELIAVIMAS

V. Bubilaitis, D. Abramavičius

Vilniaus universiteto Fizikos fakulteto Cheminės fizikos institutas, Vilnius, Lietuva

Santrauka

Įprasta molekulines sistemas tirti artutiniame režime, naudojant trikdymų teoriją, kuri leidžia apibrėžti ir pasitelkti atsako funkcijas. Tačiau jei trikdymų eilutė lėtai konverguoja (arba diverguoja), spektrinių savybių prigimtis gali būti klaidingai interpretuojama. Artutinis trikdymų teorijos režimas gali netikti esant dideliam žadinančio lauko intensyvumui. Vienas iš reiškinių, pasireiškiančių su dideliu žadinimo intensyvumu yra eksitono–eksitono anihiliacija (EEA). Tokio tipo uždavinius galima spręsti naudojant netiesines eksitonų lygtis (NEL). Kadangi tai yra begalinės lygčių hierarchijos, lygčių hierarchijos „uždarymui“ būtina arba atmesti tam tikros eilės lygčių narius, arba juos faktorizuoti, t. y. išreikšti mažesnės eilės narių sandauga. Tai gali lemti netikėtus rezultatus: lygčių sprendiniai gali diverguoti, atsirasti nefizikiniai efektai. Šiame darbe aprašomos netiesinės eksitonų lygtys su EEA nariais, naudojant skirtingas faktorizavimo schemas didelio žadinimo režime, ir kaip tai atsispindi sugerties spektre. Suskaičiuoti nuo žadinimo intensyvumo priklausantys sugerties spektrai rodo, kad dėl didelio žadinimo intensyvumo atsiranda papildomos sugerties juostos, kurių padėtis stipriai priklauso nuo žadinimo intensyvumo. Išsiaiškinta, kad spektrų elgsena labai jautri nelyginės eilės narių faktorizavimui, bet lygtyse įmanoma parinkti tokį faktorizavimo metodą, kuris atitiktų konkretų eksperimentą. EEA labai pasitarnauja stabilizuojant sprendinius, skirtumai tarp įvairių faktorizavimo schemų susilpnėja. Tokiu būdu, naudojant NEL, galima sukurti labai efektyvias modeliavimo metodikas, kurios tiktų įvairiems matavimams.